The EMBO Journal (2004) 23, 2039–2046 | © 2004 European Molecular Biology Organization | All Rights Reserved 0261-4189/04
www.embojournal.org

THE EMBO JOURNAL

NMR of α-synuclein–polyamine complexes elucidates the mechanism and kinetics of induced aggregation

Claudio O Fernández[1,*], Wolfgang Hoyer[2], Markus Zweckstetter[3], Elizabeth A Jares-Erijman[4], Vinod Subramaniam[5], Christian Griesinger[3] and Thomas M Jovin[2,*]

[1]LANAIS RMN 300, Facultad de Farmacia y Bioquímica, Universidad de Buenos Aires, Buenos Aires, Argentina, [2]Department of Molecular Biology, Max Planck Institute for Biophysical Chemistry, Göttingen, Germany, [3]Department of NMR-based Structural Biology, Max Planck Institute for Biophysical Chemistry, Göttingen, Germany, [4]Departamento de Química Orgánica, Facultad de Ciencias Exactas y Naturales, Universidad de Buenos Aires, Buenos Aires, Argentina and [5]Biophysical Engineering Group, Faculty of Science and Technology, University of Twente, Enschede, The Netherlands

The aggregation of α-synuclein is characteristic of Parkinson's disease (PD) and other neurodegenerative synucleinopathies. The 140-aa protein is natively unstructured; thus, ligands binding to the monomeric form are of therapeutic interest. Biogenic polyamines promote the aggregation of α-synuclein and may constitute endogenous agents modulating the pathogenesis of PD. We characterized the complexes of natural and synthetic polyamines with α-synuclein by NMR and assigned the binding site to C-terminal residues 109–140. Dissociation constants were derived from chemical shift perturbations. Greater polyamine charge ($+2 \rightarrow +5$) correlated with increased affinity and enhancement of fibrillation, for which we propose a simple kinetic mechanism involving a dimeric nucleation center. According to the analysis, polyamines increase the extent of nucleation by $\sim 10^4$ and the rate of monomer addition ~40-fold. Significant secondary structure is not induced in monomeric α-synuclein by polyamines at 15°C. Instead, NMR reveals changes in a region (aa 22–93) far removed from the polyamine binding site and presumed to adopt the β-sheet conformation characteristic of fibrillar α-synuclein. We conclude that the C-terminal domain acts as a regulator of α-synuclein aggregation.

The EMBO Journal (2004) **23,** 2039–2046. doi:10.1038/sj.emboj.7600211; Published online 22 April 2004
Subject Categories: structural biology; neuroscience
Keywords: amyloid; fibrillation; Parkinson's disease; spermine

*Corresponding authors. CO Fernández, Laboratorio Nacional de Resonancia Magnética, Facultad de Farmacia y Bioquímica, Universidad de Buenos Aires, Buenos Aires, Argentina. Tel.: +54 11 496 48 253; Fax: +54 11 496 48 253; E-mail: cfernand@ffyb.uba.ar or TM Jovin, Department of Molecular Biology, Max Planck Institute for Biophysical Chemistry, Am Fassberg 11, 37077 Göttingen, Germany. Tel.: + 49 551 201 1382; Fax +49 551 201 1467; E-mail: tjovin@gwdg.de

Received: 28 October 2003; accepted: 22 March 2004; published online: 22 April 2004

Introduction

The misfolding and dysfunction of α-synuclein contribute to the pathogenesis of various neurodegenerative disorders (Goedert, 2001; Dev *et al*, 2003; Dobson, 2003). The 140 aa protein is natively unstructured (Weinreb *et al*, 1996) but adopts a β-stranded conformation in the aggregated, fibrillar forms characteristic of the Lewy bodies in Parkinson's disease (Der-Sarkissian *et al*, 2003). In contrast, complexes of α-synuclein with phospholipid membranes, possibly involved in the physiological regulation of dopamine neurotransmission (Dev *et al*, 2003), exhibit a partially α-helical secondary structure (Bussell and Eliezer, 2003; Chandra *et al*, 2003). The rate of α-synuclein fibrillation is significantly accelerated by numerous environmental conditions and factors, including low pH and high temperature (Uversky *et al*, 2001a; Hoyer *et al*, 2002), organic solvents (Munishkina *et al*, 2003), heparin and other glycosaminoglycans (Cohlberg *et al*, 2002), and metal cations (Uversky *et al*, 2001c; Hoyer *et al*, 2002). The time course of fibrillation is consistent with a nucleation-dependent mechanism (Wood *et al*, 1999), presumed to involve partially folded intermediates (Uversky *et al*, 2001b) during the initial phases.

α-Synuclein forms complexes with unstructured polycations (Goers *et al*, 2003b) and the highly basic histone H1 (Goers *et al*, 2003a) and is oligomerized as a consequence. We recently reported (Antony *et al*, 2003) that the cellular polyamines putrescine, spermidine, and spermine accelerate the aggregation and fibrillation of α-synuclein to a degree that increases with the total charge, length, and concentration of the polyamine. Polyamines are cellular stabilizers of nucleic acids and membranes and as such are essential for growth and differentiation. They mediate local and systemic functions in the central nervous system and are involved in neurodegenerative processes (Morrison and Kish, 1998). At high intracellular levels, spermidine and spermine are toxic (Auvinen *et al*, 1992) and can produce oxidative intermediates during polyamine retroconversion. For these reasons, we have postulated (Antony *et al*, 2003) that at physiological concentrations and in a cellular context, these natural compounds may modulate the propensity of α-synuclein to form fibrils, thereby playing a significant role in the formation of cytotoxic, cytosolic aggregates.

In this work, we characterized the binding of the polyamines spermidine, spermine, and putrescine, and the synthetic analogs 4-4-4 and BE-4-4-4-4 (for structures see Figure 3A) to α-synuclein by NMR spectroscopy and other biophysical and biochemical techniques.

Results

Aggregation kinetics of α-synuclein monitored by thioflavin T

The time course of α-synuclein aggregation at 37°C was monitored by the standard thioflavinT (ThioT) fluorescence

assay (Figure 1A). The characteristic lag time of aggregation of the unliganded protein was reduced from >20 h to a degree dependent on the formal positive charge of the polyamines: BE-4-4-4-4 (+5) > spermine (+4) ≈ 4-4-4(+4) > spermidine (+3) > putrescine (+2). Far-UVCD spectroscopy (data not shown) did not reveal significant polyamine-induced changes in the characteristic spectrum of unstructured α-synuclein (Antony *et al*, 2003) upon saturation with spermine at 20°C.

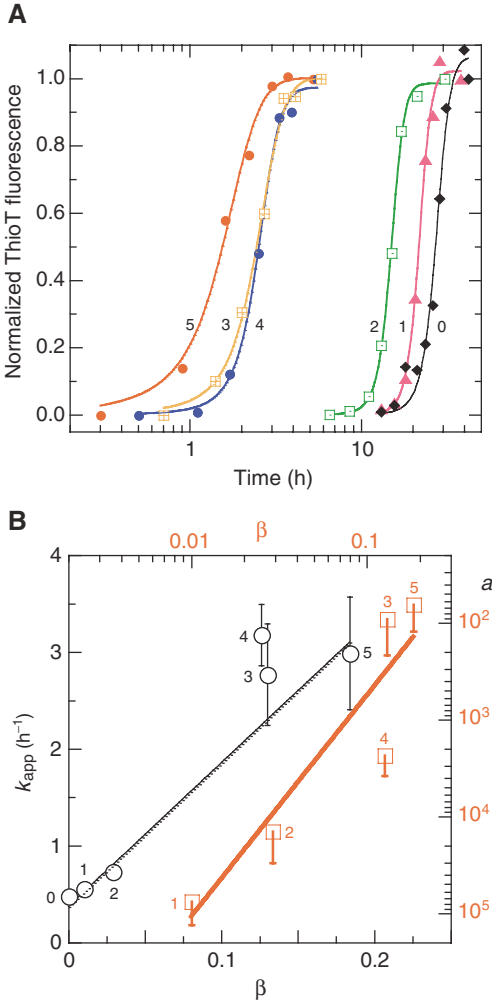

Figure 1 Aggregation kinetics at 37°C of α-synuclein ± polyamines monitored by ThioT assay. (**A**) No polyamine (0), and 100 μM putrescine (1), spermidine (2), spermine (3) and the synthetic polyamines 4-4-4 (4) and BE-4-4-4-4 (5); the numbers adjacent to the curves and points of panels A and B identify the corresponding compound. The solid lines represent fits to α[*t*] (Equation 4, including a factor for residual uncertainty in data normalization) and yielding kinetic parameters k_{app} and *a* (Equation 4) for the six cases. Conditions: 25 mM Tris–HCl, pH 7.2, 70 μM protein. (**B**) Data analysis. Black line and axes: linear regression according to Equation 4 of k_{app} versus β, the fraction of α-synuclein with bound polyamine computed with Equation 1 from the K_d values obtained from ^{15}N chemical shifts at 15°C (Figure 4A); the derived parameters are k_{agg} and γ. Red line and axes: linear regression of log[*a*] versus log[β] according to Equations 2 and 4, yielding the nucleation parameters, *n*, $K_{nco}\varepsilon$, and $K_{ncp}\varepsilon$ (see text for values). Errors in s.e. units (shown one-sided for *a*).

Characterization of α-synuclein and its polyamine complexes by ^{1}H–^{15}N HSQC NMR

NMR signals of backbone amides constitute excellent probes of complex formation, providing maps of the interaction interfaces and binding constants (Craik and Wilce, 1997). The ^{1}H–^{15}N HSQC spectrum of a 0.1 mM sample of uniformly ^{15}N-labeled α-synuclein recorded at 15°C and pH 7.4 is shown in Figure 2A. The resonances were well resolved and sharp, with a limited dispersion of chemical shifts, reflecting the unfolded nature and the high degree of backbone mobility (Bussell and Eliezer, 2001; Eliezer *et al*, 2001) of the native protein. The cross-peaks of all backbone amides in the 2D spectrum were assigned and corresponded well with previous studies (Eliezer *et al*, 2001). The titration of ^{15}N-enriched α-synuclein with polyamines was monitored by ^{1}H–^{15}N HSQC spectra, which retained the excellent resolution of the uncomplexed, native protein but demonstrated backbone chemical shift changes in a discrete number of residues located in the highly acidic Q^{109}–A^{140} C-terminal region of the protein (Figures 2B, C and 3B). No broadened or new resonances appeared. Instead, the observed displacements of the chemical shifts were continuous, monotonic functions of the polyamine concentration (Figure 4A).

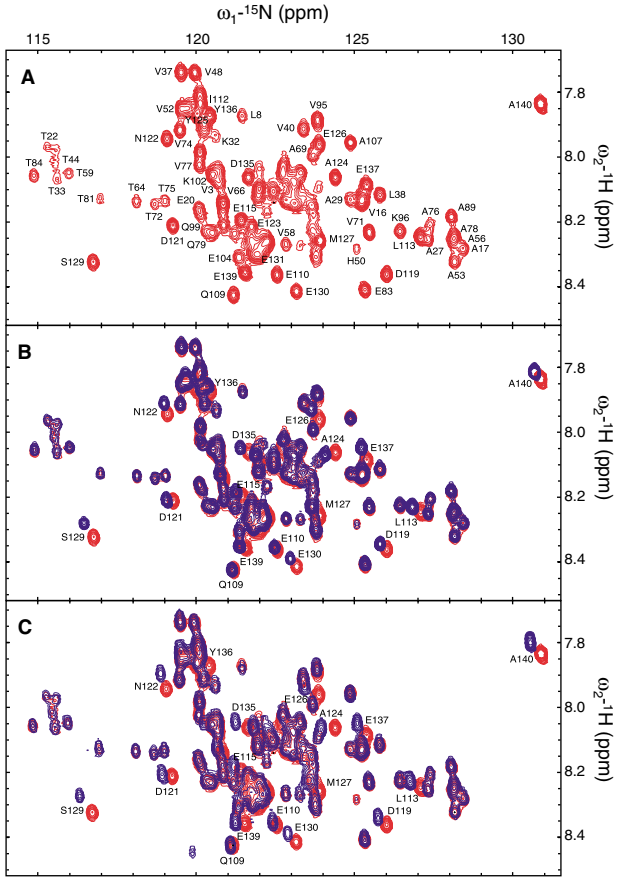

Figure 2 ^{1}H–^{15}N HSQC spectra of α-synuclein in the absence and presence of polyamines. (**A**) ^{1}H–^{15}N HSQC spectrum of 100 μM α-synuclein in 25 mM Tris–HCl and 0.1 M NaCl, pH 7.4, recorded at 15°C. Overlaid contour plots of the ^{1}H–^{15}N HSQC spectra of α-synuclein in the absence (red) and presence (blue) of 3 mM spermine (**B**) or BE-4-4-4-4 (**C**). Amino-acid residues displaying significant chemical shifts are identified.

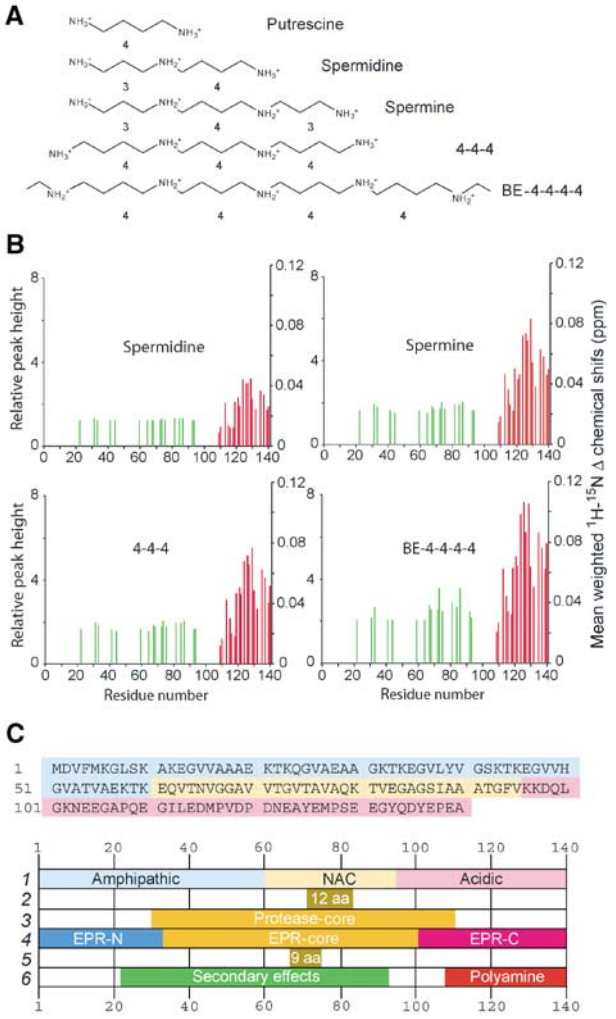

Figure 3 Polyamine structures (**A**) and changes in the mean weighted ^{1}H–^{15}N chemical shifts and selected intensities (**B**) between the ^{1}H–^{15}N HSQC spectra of free α-synuclein and α-synuclein in the presence of 3 mM polyamine. Red lines: residues undergoing chemical shift changes >0.05 ppm in the ^{15}N dimension. Green lines: residues showing changes in relative peak intensity $\geqslant 2$ in the BE-4-4-4-4 spectrum. (**C**) Primary sequence and domains ascribed to α-synuclein, in chronological order: *1* (Weinreb *et al*, 1996); *2* (Giasson *et al*, 2001); *3* (Miake *et al*, 2002); *4* (Der-Sarkissian *et al*, 2003); *5* (Du *et al*, 2003); *6* (this work).

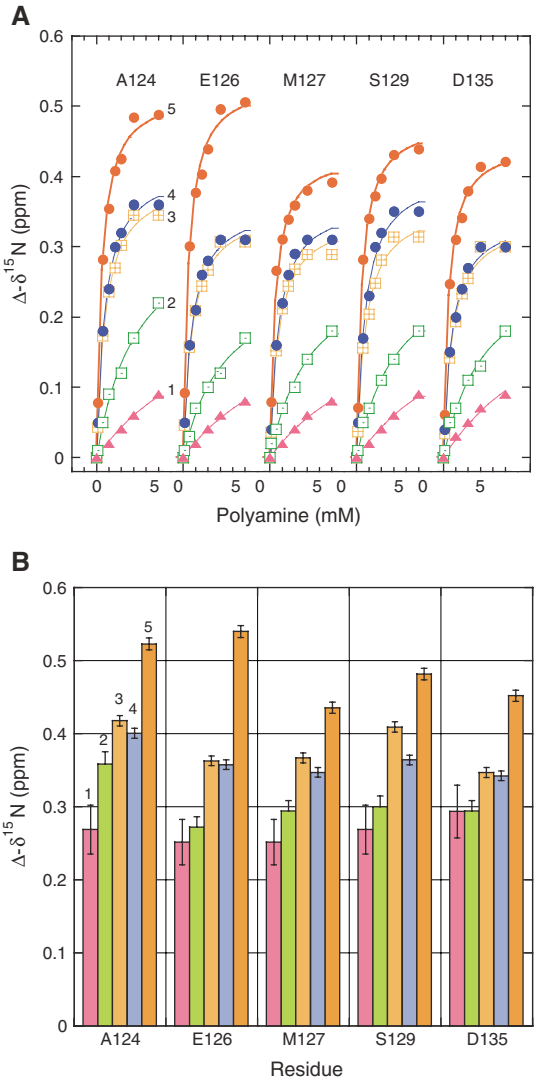

Figure 4 Binding curves of polyamines to α-synuclein (A) and derived data (B). Changes in ^{15}N chemical shifts of the indicated residues monitored by ^{1}H–^{15}N HSQC. (**A**) The different polyamines are designated as in Figure 1. Solid lines, global fits (for each polyamine, assigning the same dissociation constant K_d but different amplitudes for all residues) according to a 1:1 stoichiometry. The introduction of an additional fit parameter for a possible non-unitary complex in the analysis of the BE-4-4-4-4 data yielded a value for binding sites/α-synuclein monomer of 1.0 (albeit with poor precision). (**B**) Amplitudes (maximal values of chemical shift perturbation at saturation) derived by the fits of panel A. Errors in s.e. units.

The residues exhibiting the largest displacements in the amide resonances were A^{124}, E^{126}, M^{127}, S^{129}, and D^{135}. The five peaks were well resolved over the entire 0–5 mM polyamine concentration range and were thus well suited for the calculation of dissociation constants, K_d's (Figure 4A). Individual fits yielded values that were equal within the experimental error for the five residues and a given polyamine, justifying a global analysis (common K_d, different amplitudes; Figure 4B). The ranking of the polyamines according to their NMR-derived affinities (K_d: BE-4-4-4-4, 0.39 ± 0.02 mM; 4-4-4, 0.64 ± 0.03 mM; spermine, 0.61 ± 0.03 mM; spermidine, 3.3 ± 0.3 mM; putrescine, 10 ± 2 mM) paralleled that determined from the potentiation of aggregation. The computed amplitudes of the ligand-induced changes in chemical shifts are shown in Figure 4B. As a specificity control, α-synuclein was titrated with NH_4Cl; no significant perturbations of amide chemical shifts were observed.

NMR identification of secondary region affected by polyamine binding without formation of secondary structure

Although many peaks in the polyamine–α-synuclein complex ^{1}H–^{15}N HSQC spectra were unaltered, significant intensity changes were observed in a region (aa 22–93) far removed from the C-terminal binding site (Figure 3B), and particularly affecting threonine and glycine residues. The intensities of G$^{31, 41, 67, 68, 73, 84, 86, 93}$ and T$^{22, 33, 44, 59, 64, 72, 75, 81, 92}$ were 2–4 times that of the same residues in the spectrum of the free protein.

We further characterized the structure of the α-synuclein–spermine complex by recording the chemical shifts via an

HNCA spectrum (Supplementary data published online). The C^{α} chemical shifts did not show systematic changes (Spera and Bax, 1991) upon binding of the polyamine.

Kinetic model and analysis of polyamine-induced aggregation

The dramatic effects of polyamines on the aggregation kinetics of α-synuclein suggest a preferential involvement of the polyamine complex compared to the unliganded monomer in the nucleation and growth phases of aggregation. We incorporated this feature into a standard spontaneous nucleation-propagation polymerization mechanism, including a process of fragmentation of fibrillar/amorphous aggregates leading to a progressive increase in the number of growing points (Wegener and Savko, 1982):

Ligand binding:	ligand + monomer $\overset{K_d}{\longleftrightarrow}$ liganded monomer
Nucleation:	*n* (un)liganded monomers $\overset{K_{nc}}{\longleftrightarrow}$ nucleation center
Propagation:	(un)liganded monomers + growth centers $\overset{k_{agg}}{\longrightarrow}$ aggregated state(s)
Evolution:	mechanical fragmentation of aggregates → more growth centers

The theoretical and experimental application of this scheme requires a number of parameters and assumptions, including:

(i) the equivalence of the normalized ThioT fluorescence signal, considered to be a probe/indicator of amorphous and fibrillar structures, with the fractional monomer-to-aggregate conversion, $\alpha[t]$.

(ii) a constant fraction, β, of monomer (free or aggregated) in a polyamine-liganded form, dictated by polyamine type and concentration:

$$\beta = \frac{1 + a_1 + a_2 - \mathrm{sqrt}[(1 + a_1 + a_2)^2 - 4a_1]}{2a_1} \qquad (1)$$
$$a_1 = s_o/p_o,\ a_2 = K_d/p_o$$

where s_o is the total protein (α-synuclein) concentration, p_o is the total polyamine concentration, and K_d is the dissociation constant for a 1:1 complex. The K_d values used in the calculations were those obtained from the NMR measurements. A more elaborate version of the function β featuring a dependence on $\alpha[t]$ has also been employed to explore the consequences of a highly cooperative binding of the polyamines to aggregated forms of α-synuclein.

(iii) formation of distinct nucleation centers by the unliganded and liganded proteins via the concerted association of *n* monomer units. The concentrations nco and ncp for the unliganded and liganded protein, respectively, reflect the corresponding dissociation constants, K_{nco} and K_{ncp}:

$$\mathrm{nco} = [(1-\beta)s_o]^n/K_{nco},\quad \mathrm{ncp} = [\beta s_o]^n/K_{ncp} \qquad (2)$$

These equations, including the lack of a mixed species, incorporate approximations reflecting the experimental finding that for finite values of β,

$$\mathrm{nco} \ll \mathrm{ncp} \ll s_o,\ \text{i.e. } K_{nco} \gg K_{ncp} \gg s_o \qquad (3)$$

(iv) second-order rate constants (defined in monomer concentration units, *k* and *γk*, respectively) for the addition of the unliganded and liganded monomers to growth points. Experimentally, the dimensionless acceleration factor, γ, is $\gg 1$.

(v) a constant mean reaction cross-section for the propagation reaction, expressed as a factor ε for multiplication with the product concentration $\alpha[t]s_o$; i.e., ε is the number of monomer units/growth point. Monomer addition is assumed to be irreversible and additional rate-limiting or dead-end oligomeric intermediates are not considered. Optical and atomic force microscopy have revealed that the reactions featured under the conditions of Figure 1 lead to largely amorphous aggregates. We presume that the latter can grow by addition to a fraction or all of the constituent monomer units, a feature related but not identical to the secondary nucleation process invoked in the aggregation of islet amyloid polypeptide (Padrick and Miranker, 2003). This inference is based on simple geometrical consideration of three-dimensional structures with $\leqslant$64 units—in which all monomer units are accessible—and a key experimental requirement for efficient aggregation of α-synuclein, the continuous exposure to mechanical dispersion. The amorphous reaction mode appears to dominate for finite values of β; thus, we favor the more general term propagation to elongation for this phase of the aggregation mechanism. Under some conditions, unliganded α-synuclein forms predominantly extended fibrils. The latter propagate almost exclusively from one or both ends, such that one can envisage a progressive increase in the concentration of fibril-associated growth centers due to agitation-induced fragmentation upon attaining a critical hydrodynamic length *j*, a number estimated as 10^2–10^5 monomer units. The parameter ε (Equation 4) would be inversely proportional to *j*, accounting for the slow aggregation via a strictly fibril-extension mechanism. In contrast, mechanical dispersion of amorphous aggregates is presumed adequate for maintaining a relatively constant but large (in monomer equivalents) specific reaction cross-section. These considerations form the basis for proposing the distinct 'evolution' step in the reaction scheme.

The differential equation and solution corresponding to the above set of assumptions have the form

$$\begin{aligned}
\alpha'[t] &= k(1 + (\gamma - 1)\beta)(1 - \alpha[t])(\mathrm{nco} + \mathrm{ncp} + \varepsilon\alpha[t]s_o) \\
&\alpha[0] = 0 \\
&\alpha[t] = \frac{1 - e^{-k_{app}t}}{1 + ae^{-k_{app}t}} \qquad (4) \\
&k_{app} = k(\mathrm{nco} + \mathrm{ncp} + \varepsilon s_o)(1 + (\gamma - 1)\beta) \\
&\quad \cong k\varepsilon s_o(1 + (\gamma - 1)\beta) = k_{agg}s_o(1 + (\gamma - 1)\beta) \\
&a = \frac{\varepsilon s_o}{\mathrm{nco} + \mathrm{ncp}} = \frac{\varepsilon}{s_o^{n-1}((1-\beta)^n/K_{nco} + \beta^n/K_{ncp})} \\
&\quad \cong \frac{K_{ncp}\varepsilon}{s_o^{n-1}\beta^n} \\
&\text{at } \alpha[t_{1/2}] = 1/2: \\
&\quad t_{1/2} = \frac{\ln[a+2]}{k_{app}} \cong \frac{\ln[a]}{k_{app}} \\
&\quad \frac{\partial\alpha}{\partial t}[t_{1/2}] = \frac{k_{app}}{4}\left(\frac{a+2}{a+1}\right) \cong \frac{k_{app}}{4} \\
&\quad t_{1/2} \cdot \frac{\partial\alpha}{\partial t}[t_{1/2}] \cong \ln[a]/4
\end{aligned}$$

in which $k_{agg} = k\varepsilon$, the approximation for k_{app} derives from Equation (condition) 3, and the approximation for *a* applies for finite values of β. The general expressions for k_{app} and *a* have the correct limits at the extremes of β (0, 1). Note that

according to this scheme, the lag time, defined as $t_{1/2}$, is a function of both the thermodynamic and kinetic parameters.

The above formalism provided satisfactory two-parameter fits to the kinetic data (Figure 1A), yielding a set of k_{app} (range, 2–11 h^{-1}) and a (range, 3×10^{-6}–3×10^{-2}) values for the different polyamines. We surmised that the intrinsic rate and acceleration constants, k_{agg} and γ, respectively, and the nucleation equilibrium constant K_{ncp} might be very similar for the entire set of compounds, such that the different time courses of aggregation (Figure 1A) reflected the different fractional saturations, β, of the monomeric α-synuclein dictated by the measured binding (dissociation) constants K_d. The data conformed well to this assumption (Figure 1B); application of Equation 4 yielded universal constants for α-synuclein and its polyamine complexes: $k_{agg} = 1.5 \pm 0.2\ M^{-1}\ s^{-1}$ and $\gamma = 40 \pm 6$. The value of k_{agg} extrapolated from the polyamine data was very similar to that derived from the measurements performed in the absence of polymine, $k_{agg} = 1.9 \pm 0.3\ M^{-1}\ s^{-1}$.

Analysis of the nucleation data, most simply represented as a concerted oligomerization of n polyamine-liganded monomers (Equations 2 and 4, Figure 1B), led to $n = 2.3 \pm 0.6$ (suggesting a dimeric species) and $K_{ncp}\varepsilon = 0.7$ (range, 0.2–20) mM, a value $\sim 10^{-4}$ that for unliganded α-synuclein, $K_{nco}\varepsilon = 4$ (range, 2–30) M.

As stated in the Introduction, salt composition and concentration can profoundly influence the aggregation of α-synuclein. The NMR experiments were performed with samples containing 0.1 M NaCl, which was absent in the aggregation experiments. Thus, the latter were repeated in the presence of 0.15 and 0.2 M NaCl, yielding values of k_{app}, which were 2 ± 1-fold that in the absence of added salt; a was not affected significantly. Although comparative experiments in the presence of polyamines have not yet been performed, we conclude that the effects on the binding constants of NaCl in this 0–0.2 M concentration range are probably relatively minor.

Discussion

The NMR analysis of α-synuclein complexes with polyamines (Figure 3) indicates that the acceleration of α-synuclein aggregation–fibrillation in the presence of polyamines is a direct consequence of binding to the C-terminus of the protein. Quantitative analysis of the chemical shift data provided the equilibrium parameters for the different polyamines. The computed amplitudes of the ligand-induced changes in chemical shifts exhibited a similar pattern for five analyzed residues (Figure 4B). They increased with the charge (and thus affinity) of the polyamine, probably reflecting differences in binding dynamics and residence times. However, the patterns of the altered backbone chemical shifts mapped on the primary sequence were very similar, suggesting a common mode of binding dictated largely by electrostatic interactions generating a distribution centered near A^{124}. These results constitute the first direct demonstration of a well-defined binding interface in the C-terminal domain of α-synuclein in its native state.

The chemical shift perturbations induced by each polyamine in the primary binding site were closely correlated with the corresponding changes in peak height in the remote secondary region (Figure 3B). This finding implies that the two phenomena were linked. However, the invariance of the ^{1}H and ^{15}N chemical shifts in the aa 22–93 region and the lack of CD changes or of systematic C^{α} chemical shifts in the HNCA spectra of the polyamine complexes indicate the absence of significant conformational changes or induction of secondary structure. Nonetheless, more global domain–domain rearrangements may well occur. For example, one could hypothesize that in the unliganded 'normal' conformation, the dynamic C-terminal domain blocks the self-aggregating domain in the central core of the molecule identified by many studies (Figure 3C). C-terminal modifications, such as charge neutralization and conformational adaptation accompanying polyamine binding, might lead to a release of the self-aggregating domain, thereby promoting its transition to β-stranded filament formation. The NMR results would be reflecting the earliest molecular events at the onset of α-synuclein aggregation: the altered chemical shifts in the C-terminal domain identify the polyamine binding motif, whereas the increased intensities of resonances in the N-terminal and central region reflect changes such as increased rotational dynamics (lower τ_c) and/or disruption of other dynamic processes.

It is instructive to relate the present results to other known features of the α-synuclein system. The acidic residues in the C-terminus of α- and β-synuclein constitute a tandem repeat of 16 aa, and the entirety of this structure (aa 109–140) is involved in polyamine binding (Figure 3B). Binding of Ca^{2+} ions to the same structural motif promotes the association of α-synuclein (Nielsen *et al*, 2001). The second acidic repeat (^{125}YEMPSEEGYQDYEPEA^{140}) is important for the chaperone activity of the protein (Kim *et al*, 2002) and is implicated in aggregation and other protein–protein interactions. Modifications of other amino-acid side chains in the C-terminal domain that alter the charge distribution are also known to affect aggregation (Giasson *et al*, 2000; Fujiwara *et al*, 2002).

The secondarily affected region, comprising residues within the aa 22–93 fragment, extends beyond the amyloidogenic NAC domain and other subregions (Giasson *et al*, 2001; Uversky and Fink, 2002; Du *et al*, 2003) (Figure 4B) prone to self-aggregation and fibril formation. Indeed, our results strongly support evidence based on protease digestion (Miake *et al*, 2002) and spin labeling EPR (Der-Sarkissian *et al*, 2003) for the existence of a more extended core region ($\sim$aa 30–110) of α-synuclein (Figure 3C). The affected threonines are located within the NAC domain or within XKTKEGVXXXX repeats in the N-terminal domain. The latter decrease the tendency of α-synuclein to form β-sheet structures such as protofibrils and fibrils (Kessler *et al*, 2003) and promote lipid-bound structures likely involved in normal, as yet undetermined cellular function(s). Most of the affected glycines are embedded within the NAC region forming part of GAV or GXXX motifs (Du *et al*, 2003). The placement of glycine (small) and threonine (polar) in a more exposed hydrophobic surface as a result of polyamine binding could allow close packing as well as the facilitated formation of intermolecular side chain–side chain or side chain–backbone hydrogen bonds, thereby stabilizing alternative structures involved in the fibrillation pathway.

The primary difference between the various polyamines, the number of positive charges, is reflected in the K_d values for binding to α-synuclein, whereas the variable carbon chain

length appears to be of little or lesser importance, judging from the indistinguishability of the spermine and 4-4-4 parameters. Thus, the mechanism of polyamine-accelerated fibrillation may share features with the action of divalent (Cu^{2+}, Mn^{2+}) and trivalent (Al^{3+}, Fe^{3+}, Co^{3+}) metal ions but probably differs from that induced by acidification. As shown in this study, polyamines bind specifically to a well-defined structural motif in the C-terminus of α-synuclein, neutralizing negative charges exclusively in that region. In contrast, a decrease in pH constitutes a nonphysiological, nonspecific process affecting the charges of all titratable amino-acid side groups located in different domains of the protein. It follows that the formation of a complex between polyamines and α-synuclein, rather than the induction of a partially folded structure, represents the (a) critical step in the early stage of fibrillation of this protein in the presence of the biogenic amines.

Based on this notion, we developed and applied a simple kinetic scheme for the mechanism of α-synuclein aggregation–fibrillation, featuring distinct nucleation and growth phases (see Results). Despite the absolute minimal number of fit parameters (2), the kinetic traces of aggregation derived by the ThioT assay were fit very well, and yielded parameters indicating that the polyamines promote both steps in the reaction scheme: the nucleation to what appears to be a dimeric structure is favored $\sim 10^4$-fold and the rate of addition of the liganded protein to the aggregated species is ~ 40 times greater. In analogy to enzymatic systems and in terms of the reaction scheme introduced above, one can define a kinetic efficiency of aggregation as k/K_{nc}. Polyamines increase this parameter by a factor of $\sim 10^5$! We conclude that the C-terminal domain is an important regulator of α-synuclein aggregation.

The derived rate constants include implicitly any conformational rearrangement of the monomer required to match the growing target, which is presumed to adopt at some point in the mechanism a β-sheet configuration, for example, the parallel orientation inferred from EPR spectroscopy (Der-Sarkissian *et al*, 2003); the latter reaction may well occur in the μs or sub-μs domain (Muñoz *et al*, 1997). The conclusion that the nucleation structure consists of a dimeric species is subject to the constraints of the kinetic model but consistent with the recent report (Krishnan *et al*, 2003) of covalent (and noncovalent) dimeric forms of α-synuclein serving as transient intermediates in aggregation. Clearly, more complexity could be accommodated in the model, such as (i) allosteric stabilization of the polyamine complex in the aggregated protein, (ii) an ongoing continuous or discontinuous process of nucleation and propagation, (iii) distinct aggregation mechanisms for the unliganded and liganded α-synuclein monomer, and (iv) the possible intervention of additional, distinct reaction intermediates.

The NMR experiments reported here were neither designed to test for dimerization nor, more importantly, yielded evidence thereof. In fact, they were performed at 15°C and not at the 37°C of the aggregation assay in order to prevent aggregation of the sample, a process that would preclude the acquisition of usable spectra. Although temperature is undoubtedly a very important factor defining the equilibrium and kinetic constants for the nucleation and propagation steps of the aggregation mechanism, it is probably of lesser significance with respect to the binding of the polyamines to monomeric α-synuclein. This assertion is based on the following considerations. The analysis of the aggregation data at 37°C involved the dependence of the derived parameters on the fractional saturations, β, calculated with the K_d values derived from the NMR data at 15°C. We can anticipate that polyamine binding to the highly charged yet unstructured C-terminus of α-synuclein is characterized by significant enthalpy–entropy compensation (Williams *et al*, 1993), accounting for the relative low affinities (ΔG_{ass}, -11 to $-19\,kJ\,mol^{-1}$). That is, excluding free energy contributions of conformational strain and van der Waals interactions, which remain indeterminate in the absence of detailed structural information, the exothermic terms rising from the hydrophobic effect (desolvation) and hydrogen bonding would be balanced by the entropic loss inherent to biomolecular association reactions. The increment per positive charge in the magnitude of the free energy of association, $\Delta\Delta G$, equalled $2.9 \pm 0.4\,kJ\,mol^{-1}$, considerably less than $\sim 9\,kJ\,mol^{-1}$ for binding to DNA (Stewart and Gray, 1992), a polyanionic target with a much higher charge density. We infer that ΔH for the polyamine–synuclein binding reaction may be relatively small, and note in addition that the computed values of $\partial \log[\beta]/\partial \log[a_2]$ (Equation 1) under the conditions of our experiments were similar for the different polyamines, varying from -0.95 for spermidine to -0.71 for BE-4-4-4-4. Thus, even if we assume (unrealistically) a $\Delta H = 1.5\Delta G$, the relative decrease in β upon undergoing a $15 \rightarrow 37$°C temperature shift would vary little between spermidine (44%) and BE-4-4-4-4 (49%). We conclude that any temperature-dependent changes in K_d should have been moderate and without significant effects on the data regressions of Figure 1B. As stated above, we reached a similar conclusion with respect to the possible influence of 0.1 M NaCl on one of the two determinations (NMR, aggregation kinetics).

The investigations featured above are being extended by use of other NMR and complementary biophysical techniques applied to mutant proteins and selected peptide sequences. In particular, we are devising means for elucidating the distribution and nature of early conformational and aggregation intermediates, including the proposed dimeric nucleation center. However, the approaches and conclusions developed in the course of this study have by themselves implications for the generation of agents designed to impede or reverse the pathologic aggregation of α-synuclein and other amyloidogenic proteins (Cohen and Kelly, 2003).

Materials and methods

Materials

Unlabeled α-synuclein was expressed and purified as previously described (Hoyer *et al*, 2002). ^{15}N- and $^{13}C/^{15}N$-labeled α-synuclein was prepared from *Escherichia coli* cultures grown in M9 minimal medium supplemented with ^{15}N-H_4Cl and ^{13}C-D-glucose (Cambridge Isotope Laboratories). Natural polyamines were obtained from Sigma. The 4-4-4 and BE-4-4-4-4 derivatives were synthesized as described (Samejima *et al*, 1984).

Kinetics of α-synuclein aggregation

The aggregation of α-synuclein was carried out in solutions of 70 μM protein in 25 mM Tris–HCl, pH 7.2, ±100 μM of the individual polyamines. A measure of 300 μl of freshly prepared protein solution was incubated at 37°C in glass vials under constant mixing with micro-stirring bars. Aliquots (7.5 μl) were withdrawn at different times and added to 2 ml of 5 μM ThioT in 50 mM

Na-glycine, pH 8.2. The final protein concentration was 0.26 μM. ThioT fluorescence was excited at 446 nm and the emission at 480 nm was recorded with a Varian Cary Eclipse spectrofluorimeter. Kinetic aggregation traces were generated from time points of ThioT emission, corrected for the contribution of free dye and normalized by the final values. The parameters (k_{app} and a, Equation 4) derived from duplicate experiments were averaged. The data were analyzed with the commercial program Kaleidagraph (see text for discussion).

NMR measurements

NMR spectra were acquired at 15°C on a Bruker Avance 600 NMR spectrometer using a triple-resonance cryoprobe equipped with *z*-axis self-shielded gradient coils. Aggregation did not occur under these conditions of low temperature and absence of stirring. All NMR experiments were performed with pulsed-field gradient enhanced pulse sequences on a 100 μM sample of α-synuclein in 25 mM Tris–HCl (pH 7.4) and 0.1 M NaCl.

Two-dimensional ^{1}H–^{15}N HSQC experiments were used for the polyamine titration series. The spectra were recorded using 256×1024 complex data points in F_1 and F_2 dimensions with 16 scans per increment and a relaxation delay of 1.2 s. The spectral widths were 1650 and 5500 Hz in the ^{15}N and ^{1}H dimensions, respectively. Titrations were performed by stepwise addition of 5 μl of concentrated stock solutions of polyamines prepared as chloride salts. Mean weighted chemical shift displacements (Figure 3B) were calculated as $[(\Delta\delta^{1}H)^2 + (\Delta\delta^{15}N)^2/25]^{1/2}$. Three-dimensional HNCA, HNCACB, and CBCA(CO)NH experiments were performed to check and facilitate backbone assignments (Bax and Grzesiek, 1993). The spectra were acquired with 1024 complex data points in the direct dimension and 24 and 60 complex data points in the N and C dimension, respectively. The spectral widths were 8992 Hz (^{1}H), 1429 Hz (^{15}N), 9433 Hz (C^{α}, C^{β}), and 3750 Hz (C^{α}). All acquired spectra were processed with XWIN-NMR and NMRPipe. Visualization and manipulation were performed with the public domain graphics program Sparky 3.

Supplementary data

Supplementary data are available at *The EMBO Journal* Online.

Acknowledgements

This work was supported by the Max Planck Society and the Fonds der Chemischen Industrie. We are indebted to Marc Baldus and Henrike Heise for useful discussions. COF was the recipient of a short-term visiting scientist fellowship from the Alexander v Humboldt Foundation. COF and EAJ-E thank Fundación Antorchas for financial support. WH gratefully thanks the Stiftung Stipendien-Fonds des Verbandes der Chemischen Industrie and the Bundesministerium für Bildung und Forschung. MZ is the recipient of a DFG Emmy Noether Fellowship (ZW 71/1–3). This work was within the scientific scope of the German Research Council Center for Molecular Physiology of the Brain (CMPB) in Göttingen, of which the Department of Molecular Biology (TMJ) is a participating member as well as the Graduiertenkolleg 782 of the German Research Council (DFG).

References

Antony T, Hoyer W, Cherny D, Heim G, Jovin TM, Subramaniam V (2003) Cellular polyamines promote the aggregation of α-synuclein. *J Biol Chem* **278:** 3235–3240

Auvinen M, Passinen A, Andersson LC, Holtta E (1992) Ornithine decarboxylase activity is critical for cell transformation. *Nature* **360:** 355–358

Bax A, Grzesiek S (1993) Methodological advances in protein NMR. *Accounts Chem Res* **26:** 131–138

Bussell Jr R, Eliezer D (2001) Residual structure and dynamics in Parkinson's disease-associated mutants of α-synuclein. *J Biol Chem* **276:** 45996–46003

Bussell R, Eliezer D (2003) A structural and functional role for 11-mer repeats in α-synuclein and other exchangeable lipid binding proteins. *J Mol Biol* **329:** 763–778

Chandra S, Chen X, Rizo J, Jahn R, Sudhof TC (2003) A broken α-helix in folded α-synuclein. *J Biol Chem* **278:** 15313–15318

Cohen FE, Kelly JW (2003) Therapeutic approaches to protein-misfolding diseases. *Nature* **426:** 905–909

Cohlberg JA, Li J, Uversky VN, Fink AL (2002) Heparin and other glycosaminoglycans stimulate the formation of amyloid fibrils from α-synuclein *in vitro*. *Biochemistry* **41:** 1502–1511

Craik DJ, Wilce JA (1997) Studies of protein–ligand interactions by NMR. *Methods Mol Biol* **60:** 195–232

Der-Sarkissian A, Jao CC, Chen J, Langen R (2003) Structural organization of α-synuclein fibrils studied by site-directed spin labeling. *J Biol Chem* **278:** 37530–37535

Dev KK, Hofele K, Barbieri S, Buchman VL, van der Putten H (2003) Part II: α-synuclein and its molecular pathophysiological role in neurodegenerative disease. *Neuropharmacology* **45:** 14–44

Dobson CM (2003) Protein folding and misfolding. *Nature* **426:** 884–890

Du H-N, Tang L, Luo X-Y, Li H-T, Hu J, Zhou J-W, Hu H-Y (2003) A peptide motif consisting of glycine, alanine, and valine is required for the fibrillization and cytotoxicity of human α-synculein. *Biochemistry* **42:** 8870–8878

Eliezer D, Kutluay E, Bussell Jr R, Browne G (2001) Conformational properties of α-synuclein in its free and lipid-associated states. *J Mol Biol* **307:** 1061–1073

Fujiwara H, Hasegawa M, Dohmae N, Kawashima A, Masliah E, Goldberg MS, Shen J, Takio K, Iwatsubo T (2002) α-Synuclein is phosphorylated in synucleinopathy lesions. *Nat Cell Biol* **4:** 160–164

Giasson BI, Duda JE, Murray IVJ, Chen Q, Souza JM, Hurtig HI, Ischiropoulos H, Trojanowski JQ, Lee VMY (2000) Oxidative damage linked to neurodegeneration by selective α-synuclein nitration in synucleinopathy lesions. *Science* **290:** 985–989

Giasson BI, Murray IVJ, Trojanowski JQ, Lee VMY (2001) A hydrophobic stretch of 12 amino acid residues in the middle of α-synuclein is essential for filament assembly. *J Biol Chem* **276:** 2380–2386

Goedert M (2001) Alpha-synuclein and neurodegenerative diseases. *Nat Rev Neurosci* **2:** 492–501

Goers J, Manning-Bog AB, McCormack AL, Millett IS, Doniach S, Di Monte DA, Uversky VN, Fink AL (2003a) Nuclear localization of α-synuclein and its interaction with histones. *Biochemistry* **42:** 8465–8471

Goers J, Uversky VN, Fink AL (2003b) Polycation-induced oligomerization and accelerated fibrillation of human α-synuclein *in vitro*. *Protein Sci* **12:** 702–707

Hoyer W, Antony T, Cherny D, Heim G, Jovin TM, Subramaniam V (2002) Dependence of α-synuclein aggregate morphology on solution conditions. *J Mol Biol* **322:** 383–393

Kessler JC, Rochet JC, Lansbury Jr PT (2003) The N-terminal repeat domain of α-synuclein inhibits β-sheet and amyloid fibril formation. *Biochemistry* **42:** 672–678

Kim TD, Paik SR, Yang CH (2002) Structural and functional implications of C-terminal regions of α-synuclein. *Biochemistry* **41:** 13782–13790

Krishnan S, Chi EY, Wood SJ, Kendrick BS, Li C, Garzon-Rodriguez W, Wypych J, Randolph TW, Narhi LO, Biere AL, Citron M, Carpenter JF (2003) Oxidative dimer formation is the critical rate-limiting step for Parkinson's disease α-synculein fibrillogenesis. *Biochemistry* **42:** 829–837

Miake H, Mizusawa H, Iwatsubo T, Hasegawa M (2002) Biochemical characterization of the core structure of α-synuclein filaments. *J Biol Chem* **277:** 19213–19219

Morrison LD, Kish SJ (1998) Ornithine decarboxylase in human brain: influence of aging, regional distribution, and Alzheimer's disease. *J Neurochem* **71:** 288–294

Munishkina LA, Phelan C, Uversky VN, Fink AL (2003) Conformational behavior and aggregation of α-synuclein in organic solvents: modeling the effects of membranes. *Biochemistry* **42:** 2720–2730

Muñoz V, Thompson PA, Hofrichter J, Eaton WA (1997) Folding dynamics and mechanism of β-hairpin formation. *Nature* **390:** 196–199

Nielsen MS, Vorum H, Lindersson E, Jensen PH (2001) Ca^{2+} binding to α-synuclein regulates ligand binding and oligomerization. *J Biol Chem* **276:** 22680–22684

Padrick SB, Miranker AD (2003) Islet amyloid: phase partitioning and secondary nucleation are central to the mechanism of fibrillogenesis. *Biochemistry* **41:** 4694–4703

Samejima K, Takeda Y, Kawase M, Okada M, Kyogoku Y (1984) Syntheses of ^{15}N-enriched polyamines. *Chem Pharm Bull* **32:** 3428–3435

Spera S, Bax A (1991) Empirical correlation between protein backbone conformation and C^{α} and C^{β} ^{13}C nuclear magnetic resonance chemical shifts. *J Am Chem Soc* **113:** 5490–5492

Stewart KD, Gray TA (1992) Survey of the DNA binding properties of natural and synthetic polyamino compounds. *J Phys Org Chem* **5:** 461–466

Uversky VN, Fink A (2002) Amino acid determinants of α-synuclein aggregation: putting together pieces of the puzzle. *FEBS Lett* **522:** 9–13

Uversky VN, Lee HJ, Li J, Fink AL, Lee SJ (2001a) Stabilization of partially folded conformation during α-synuclein oligomerization in both purified and cytosolic preparations. *J Biol Chem* **276:** 43495–43498

Uversky VN, Li J, Fink AL (2001b) Evidence for a partially folded intermediate in α-synuclein fibril formation. *J Biol Chem* **276:** 10737–10744

Uversky VN, Li J, Fink AL (2001c) Metal-triggered structural transformations, aggregation, and fibrillation of human α-synuclein—a possible molecular link between Parkinson's disease and heavy metal exposure. *J Biol Chem* **276:** 44284–44296

Wegener A, Savko P (1982) Fragmentation of actin filaments. *Biochemistry* **21:** 1909–1913

Weinreb PH, Zhen W, Poon AW, Conway KA, Lansbury Jr PT (1996) NACP, a protein implicated in Alzheimer's disease and learning, is natively unfolded. *Biochemistry* **35:** 13709–13715

Williams DH, Searle MS, Mackay JP, Gerhard U, Maplestone RA (1993) Toward an estimation of binding constants in aqueous solution: studies of associations of vancomycin group antibiotics. *Proc Natl Acad Sci USA* **90:** 1172–1178

Wood SJ, Wypych J, Steavenson S, Louis JC, Citron M, Biere AL (1999) α-Synuclein fibrillogenesis is nucleation-dependent—implications for the pathogenesis of Parkinson's disease. *J Biol Chem* **274:** 19509–19512

